Atmos. Meas. Tech. Discuss., https://doi.org/10.5194/amt-2018-408
Manuscript under review for journal Atmos. Meas. Tech.
Discussion started: 10 December 2018

Atmospheric Measurement Techniques Discussions

A novel study of the morphology and effective density of externally mixed black carbon aerosols in ambient air using a size-resolved single-particle soot photometer (SP2)

Yunfei Wu[1*], Yunjie Xia[1, 2], Rujin Huang[3], Zhaoze Deng[4], Ping Tian[5], Xiangao Xia[4], Renjian Zhang[1*]

1 Key Laboratory of Regional Climate-Environment for Temperate East Asia (RCE-TEA), Institute of Atmospheric Physics, Chinese Academy of Sciences, Beijing 100029, China

2 University of Chinese Academy of Sciences, Beijing, 100049, China

3 Key Laboratory of Aerosol Chemistry and Physics, State Key Laboratory of Loess and Quaternary Geology, Institute of Earth and Environment, Chinese Academy of Sciences, Xi'an 710061, China

4 Key Laboratory of Middle Atmosphere and Global Environment Observation (LAGEO), Institute of Atmospheric Physics, Chinese Academy of Sciences, Beijing 100029, China

5 Beijing Weather Modification Office, Beijing 100089, China

Correspondence to: Yunfei Wu (wuyf@mail.iap.ac.cn) and Renjian Zhang (zrj@mail.iap.ac.cn)

Abstract

The morphology of externally mixed black carbon (*ext*BC) aerosols, an important factor affecting radiative forcing, was studied by a tandem method coupling a differential mobility diameter (DMA) with a single-particle soot photometer (SP2). Ambient particles were selected by the DMA, and the size-resolved *ext*BC particles were distinguished from those of a thick coating (internally mixed) and quantified by the SP2. Time differences between the DMA size selection and the SP2 measurement were processed previously, as well as the effects of multicharged particles. Based on the mass-mobility relationship, the fractal dimension of the *ext*BC particles was obtained, with a value of 2.36±0.04. This value is comparable with those of diesel exhaust particles, implying a predominant contribution of vehicle emissions to the ambient *ext*BC in urban Beijing. The effective densities (ρ_{eff}) of the *ext*BC in the mobility diameter range of 140–750 nm were also derived, with values gradually decreasing

Atmos. Meas. Tech. Discuss., https://doi.org/10.5194/amt-2018-408
Manuscript under review for journal Atmos. Meas. Tech.
Discussion started: 10 December 2018

Atmospheric Measurement Techniques Discussions

from 0.34 g cm^{-3} at 140–160 nm to 0.12 g cm^{-3} at 700 nm. The ρ_{eff} values were generally lower than those measured using the DMA-aerosol particle mass analyzer (APM) system. This was most likely due to the lower BC masses determined by the SP2 compared to those from the APM, since the SP2 measured the mass of pure refractory BC instead of the entire BC aggregate consisting of both refractory BC and nonrefractory components measured by the APM.

1 Introduction

Black carbon (BC), a byproduct of incomplete combustion, is the main light-absorbing component in atmospheric aerosols. BC can lead to positive radiative forcing only second to CO_2 and thus Earth warming (IPCC, 2013). However, there remains a large amount of uncertainty regarding the radiative forcing induced by BC due to its complexity and variability in the morphology, mixing state and hygroscopicity. Freshly emitted BC particles usually exhibit chain-like agglomerates built up by a number of primary carbon spherules (Park et al., 2004), which are generally hydrophobic. Condensation of organic and/or inorganic components lead to a collapse of the chain-like agglomerates, and in turn, a compact structure of BC particles (Slowik et al., 2007; Zhang et al., 2008). Changes in the morphology of BC particles affect their optical properties. Meanwhile, encasement by organic and/or inorganic coatings also increases the absorption of BC particles through the lensing effect (Shiraiwa et al., 2010; Peng et al., 2016). In addition, water-soluble coatings increase the hydrophilic ability of the BC particles (Zhang et al., 2008; McMeeking et al., 2011), indirectly affecting the radiative forcing by affecting the cloud processes.

Laboratory studies indicate that freshly emitted BC particles can be thickly coated within a few hours in the atmosphere (Pagels et al., 2009; Peng et al., 2016). Thus, many studies have focused on the optical properties and radiative forcing of thickly-coated BC particles (Jacobson, 2001; Khalizov et al., 2009; Liu et al., 2017). However, *in situ* measurements have shown that a great number of uncoated and/or thinly-coated BC particles exist in the ambient atmosphere, with a fraction even higher than that of the aged BC particles (Schwarz et al., 2008). In general, thickly-coated BC particles

Atmos. Meas. Tech. Discuss., https://doi.org/10.5194/amt-2018-408
Manuscript under review for journal Atmos. Meas. Tech.
Discussion started: 10 December 2018

account for <50% of the BC-containing particles in urban areas based on single-particle soot photometer (SP2) measurements (Huang et al., 2012; Wang et al., 2014; Wu et al., 2016). The existence of a large fraction of uncoated BC particles is likely due to continuous emission from combustion processes such as vehicle exhaust. Therefore, studies on the radiative forcing of BC particles without thick coatings are also essential, especially in urban areas. First, the morphologies and sizes of these quasi-bare BC particles should be investigated, as they greatly impact the optical properties of the particles.

The morphology of agglomerate BC particles is often studied directly using transmission electron microscopy (TEM) (Park et al., 2004). However, the timeliness and representation of filter-based TEM measurements is challenged because only a small fraction of particles on the filter collected during a considerable period are investigated (Wentzel et al. 2003). By comparison, online tandem techniques can provide much more efficient and representative measurements of particle properties, including morphology (Park et al., 2008). For example, based on the measurements of an electrical low-pressure impactor (ELPI) or an aerosol particle mass analyzer (APM) in tandem with a differential mobility analyzer (DMA), the fractal dimension, a crucial representative aspect of the morphology of agglomerate BC particles, has been studied (Park et al., 2003; Maricq and Xu, 2004; Olfert et al., 2007; Rissler et al., 2014). The effective density and the dynamic shape factor of these agglomerates can also be obtained from tandem measurements. Generally, a condensation particle counter (CPC) connected to an APM is used to obtain the typical mass of the size-selected particles from the DMA, which is determined as the mass corresponding to the peak APM voltage that results in the maximum particle number concentration. There exist large uncertainties from CPC detection when the particle concentration is low. Thus, the DMA-APM measurement is usually limited to relatively small particles that are abundant in the atmosphere (Geller et al., 2006). The upper size limit of the measured particles using the DMA-APM system is generally not larger than 400 nm in mobility diameter (Park et al., 2003; Maricq and Xu, 2004; Olfert et al., 2007; Rissler et al., 2014).

Atmos. Meas. Tech. Discuss., https://doi.org/10.5194/amt-2018-408
Manuscript under review for journal Atmos. Meas. Tech.
Discussion started: 10 December 2018

The SP2 developed on the basis of the laser-induced incandescence technique was widely used to study BC aerosol properties. It determines the BC mass from particle to particle with very high precision and accuracy and distinguishes the BC aggregates with or without thin coatings from the thickly-coated BC particles (Schwardz et al., 2006; Moteki and Kondo, 2007). In this study, we developed a system consisting of an SP2 connected in tandem with the DMA. This system was used to study the morphology of the BC aggregates from ~100 nm to 750 nm in mobility diameter. An advantage of this system is that the SP2 measures the mass of pure BC instead of the entire mass of the BC-containing particles that was determined using the APM or ELPI in previous studies, leading to a more accurate detection of the effective density of the BC aggregates. Meanwhile, the size limitation for BC aggregate detection is expanded to 750 nm in mobility diameter, providing more comprehensive knowledge on the morphology of the BC aggregates in ambient air. Using this novel tandem system, the fractal dimension, effective density and dynamic shape factor of ambient BC aggregates were investigated, providing important insights for better assessment of the regional radiative effects of agglomerate BC particles.

2 Methodology

2.1 Experimental setup

The tandem system comprises a size selection unit and a measurement section. As shown in Fig. 1, a sample of air was drawn through the size selection unit (a DMA, model 3081, TSI Inc.) to generate quasi-monodisperse particles with a certain electrical mobility diameter. The size-selected particles were delivered to the measurement section for analysis by various methods, including an SP2 (Droplet Measurement Technologies), a CPC (model 3776, TSI Inc.) and two microaethalometers (model AE51, Aethlab). The operational flow rates were set to 0.1, 0.3 and 0.15 LPM (STP) for the SP2, CPC and AE51, respectively. The sheath flow ratio was set to 3 LPM, resulting in a ratio of sheath to sample flow rate of 4.3:1 for the DMA. Particles in the range of 15–750 nm in mobility diameter can be selected. The flow rate for each instrument was calibrated using a soap film flowmeter (model Gilian Gilibrator-2

Atmos. Meas. Tech. Discuss., https://doi.org/10.5194/amt-2018-408
Manuscript under review for journal Atmos. Meas. Tech.
Discussion started: 10 December 2018

Sensidyne) before the experiment to ensure the accuracy of the selected particle sizes and measurements. This study mainly describes and discusses the DMA-SP2 measurement.

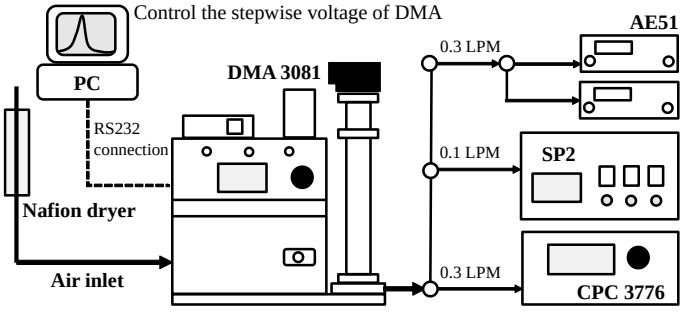

Fig. 1 Schematic of the experimental setup for size-resolved measurements of black carbon

2.2 Particle size selection

An ambient experiment was conducted on the roof of a building (approximately 8 m above the ground) on the campus of the Institute of Atmospheric Physics, Chinese Academy of Sciences (IAP, CAS) during the winter period from 23 January to 10 February 2018 (19 days in total). The site is located in an urban area of Beijing. It is a few hundred meters away from two main roads and thus may be significantly affected by vehicle emissions. More information about the measurement site is described in previous studies (e.g., Wu et al., 2016, 2017). The ambient air was dried by passing through a nafion dryer (model MD-700, Perma Pure LLC) before entering the system. The DMA was connected to an external computer on which a program was run to control the voltage of the DMA, i.e., the particle mobility diameter. Thirty-three mobility diameters were set in the program to cyclically control the particles selected by the DMA gradually increasing from 20 nm to 750 nm. Stepwise size selection repeated until the operator stopped the program. A short cycle with each of the 33 diameters lasting for 18 s and a long cycle with each size lasting for 36 s were set to alternately operate in this experiment (Fig. S2). The purpose of this setting was to

Atmos. Meas. Tech. Discuss., https://doi.org/10.5194/amt-2018-408
Manuscript under review for journal Atmos. Meas. Tech.
Discussion started: 10 December 2018

identify the time difference between the size selection and the subsequent measurement, as described in the following sections.

2.3 Black carbon measurement

The individual particulate BC mass was measured by the SP2 according to the incandescence signal when the BC passed through the intense Nd:YAG intracavity continuous laser beam (Schwardz et al., 2006). If a BC particle is coated with nonrefractory components, the coating will evaporate before the BC core incandesces, leading to a time lag between the peaks of incandescence and scattering signals that are synchronously detected by the SP2 (Moteki and Kondo, 2007). According to the frequency of the time lag, there was a significant distinction between thickly-coated (i.e., internally mixed) BC particles and thinly-coated or uncoated (i.e., externally mixed) ones (Fig. S1). BC-containing particles with a time lag shorter than 2 μs were identified as externally mixed. The time delay threshold might vary slightly from one SP2 to another, e.g., Zhang et al. (2016) reported a short time lag of 1.6 μs. However, it should be constant for a given instrument. In previous measurements using the same SP2 employed in this study, the critical time lag was maintained at 2 μs regardless of the ambient conditions, such as the pollution level (Wu et al., 2016, 2017). Before the experiment, the incandescence signal was calibrated using DMA-selected monodisperse Aquadag particles. The effective density of Aquadag was reported by Gysel et al. (2011). Since the incandescence signal is more sensitive to Aquadag, the peak intensity of the incandescence signal was reduced by a factor of 25% when calculating the calibration coefficient (Laborde et al., 2012). The calibration was performed again after the experiment to ensure the stability of the measurement during the entire experiment.

2.4 Theoretical calculation of the morphology and effective density

The structure of the externally mixed BC (*ext*BC), agglomerated by primary spherules with diameters of 20-60 nm (Alexander et al., 2008), can be characterized by a mathematical parameter, the fractal dimension (D_f), which is approximately expressed

Atmos. Meas. Tech. Discuss., https://doi.org/10.5194/amt-2018-408
Manuscript under review for journal Atmos. Meas. Tech.
Discussion started: 10 December 2018

as a power law relationship between the mass of the agglomerate particle (m) and its mobility diameter (d_{mob}), expressed as

$$m = k \cdot d_{mob}^{D_f}$$

where k is a constant. It should be noted that the approximation is applied only when the D_f is greater than 2, the regime in which the *ext*BC particles are generally located (Park et al., 2003). The D_f value of a sphere is 3. Thus, a particle is closer and closer to a sphere if the D_f increases gradually to 3.

The effective density (ρ_{eff}) of the *ext*BC particles is calculated as the ratio of the BC mass (m) measured using the SP2 and its volume based on the mobility diameter selected by the DMA, expressed as

$$\rho_{eff} = \frac{6m}{\pi d_{mob}^3}$$

Combining Eq. 1 and 2, ρ_{eff} can also be expressed as a function of d_{mob},

$$\rho_{eff} = K \cdot d_{mob}^{D_f-3}$$

The dynamic shape factor is also calculated to indicate the morphology of the *ext*BC particles. It is derived from the ratio of the slip-corrected mass equivalent diameter (d_{me}) and d_{mob}, expressed as

$$\chi = \frac{d_{mob} \cdot C_c(d_{me})}{d_{me} \cdot C_c(d_{mod})}$$

where d_{me} is calculated from the BC mass (m) by assuming the BC particle to be a compact sphere with density 1.8 g cm^{-3}, and C_c is the Cunningham slip correction factor parameterized by particle diameter (d)

$$C_c(d) = 1 + \frac{2\lambda}{d}[\alpha + \beta \exp(-\frac{\gamma \cdot d}{2\lambda})]$$

where λ is the mean free path of the gas molecules, which is set to 65 nm in this study according to Zhang et al. (2016). The values of the three empirical parameters α, β and γ are 1.257, 0.4 and 1.1, respectively (Eq. 9.34 at Page 407 in Seinfeld and Pandis, 2006).

3 Data processes

3.1 Identifying the time difference between size selection and the SP2 measurement

Atmos. Meas. Tech. Discuss., https://doi.org/10.5194/amt-2018-408
Manuscript under review for journal Atmos. Meas. Tech.
Discussion started: 10 December 2018

There exists a considerable difference between the time recorded by the size selection program and that recorded by the SP2, due to the time cost of the particles transmitting from the DMA to the SP2, as well as the system clock difference between the computer on which the size selection program runs and that for the SP2 data acquisition. As shown in Fig. S2, the SP2 measurement is significantly later than the size selection.

There are two methods to identify the time difference. The first method is to find the time difference between the local peak in the particle number concentration (including both scattering and incandescence) detected by the SP2 and the beginning of the corresponding size selection cycle. During the experiment, stepwise size selection was cyclically operated to produce quasi-monodisperse particles with sizes gradually increasing from 20 nm to 750 nm. Thus, at the beginning of each new cycle, the voltage of the DMA should first drop drastically from a high value to a low one to make the particle size decrease from 750 nm to 20 nm. As a result, some particles with sizes in the SP2 efficiently detectable range (~100–500 nm) would be measured during the descent period, producing a local peak in the number concentration. Since it takes only several seconds for the descent, identifying the occurrence time of the local peak position in the SP2 clock and the beginning time of the size selection in the external computer clock will provide the time difference of each cycle. This method was utilized in this study.

The other method is to check the consistency of the number and/or mass size distributions between the short-duration cycle and long-duration cycle. Although the durations of each size in the short cycle and long cycle are different (18 s vs. 36 s), the time difference between size selection and the SP2 measurement should be uniform for adjacent short and long cycles. Setting an initial time difference and calculating the mean number and/or mass concentration of each particle size, the number and/or mass size distributions are obtained. Then, the correlation coefficients between the size distributions during short and long cycles are calculated. Changing the time difference gradually, we can obtain a set of correlation coefficients as a function of the time differences. The time difference resulting in a maximum correlation coefficient was considered as the difference between the size selection and the SP2 measurement.

Atmos. Meas. Tech. Discuss., https://doi.org/10.5194/amt-2018-408
Manuscript under review for journal Atmos. Meas. Tech.
Discussion started: 10 December 2018

Atmospheric Measurement Techniques Discussions

231

232 **3.2 Minimizing the multicharged particles**

233 The typical mass of *ext*BC at a given d_{mob} was affected by multicharged particles,
234 especially in the size range of 100–400 nm (Ning et al., 2013). If the simple average of
235 the individual *ext*BC masses at a given d_{mob} was employed, the typical *ext*BC mass
236 would be overestimated, resulting in measurement bias in the morphology of the *ext*BC
237 particles, such as an overestimation in ρ_{eff} and an underestimation in χ. Thus, following
238 the approach in the SP2 calibration process, Gaussian fitting was performed for the
239 frequency of *ext*BC mass at each d_{mob}. The major peak mass was considered as the mass
240 of singly charged *ext*BC particles corresponding to the given d_{mob} (Fig. 2). Due to the
241 detection limit of the SP2 for small BC particles with masses lower than ~0.3 fg, only
242 the frequency of the *ext*BC mass with sizes larger than 125 nm in d_{mob} could be fit by a
243 Gaussian function. Thus, the typical *ext*BC masses at sixteen d_{mob} in the range of 140–
244 750 nm were obtained, as shown in Fig. 2 and Fig. 3.

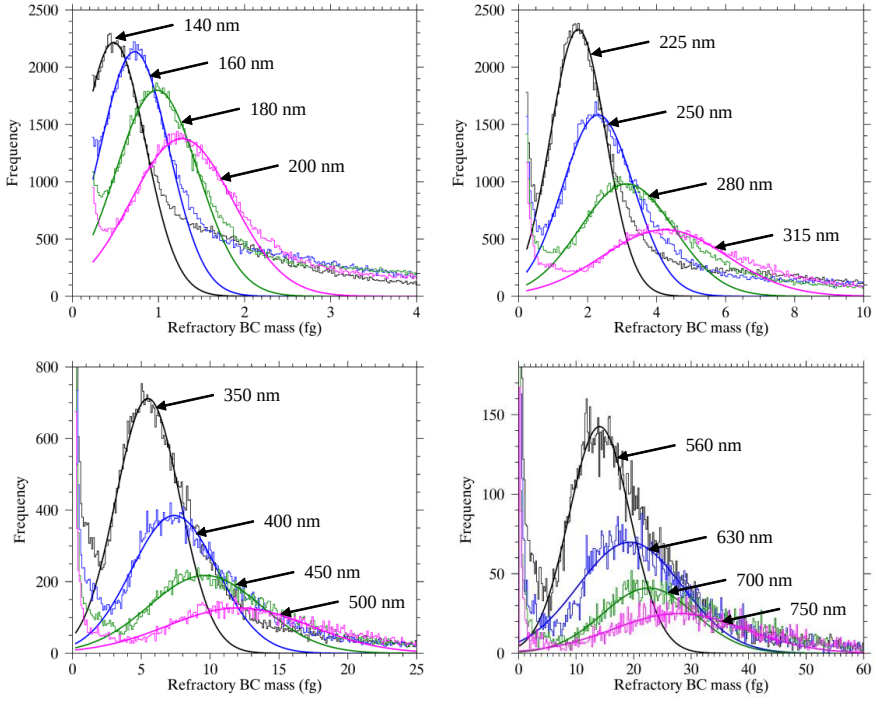

245

246 Fig. 2 Frequency distribution of the mass of the *ext*BC particles selected at different

Atmos. Meas. Tech. Discuss., https://doi.org/10.5194/amt-2018-408
Manuscript under review for journal Atmos. Meas. Tech.
Discussion started: 10 December 2018

mobility diameters. Gaussian fitting was applied to the major peak of each distribution to deliver the representative *ext*BC mass for a certain mobility diameter.

4 Results and discussion

4.1 Fractal dimension of the ambient *ext*BC

A power law relationship was applied to the d_{mob}-determined *ext*BC mass values, delivering the fractal dimension (D_f) of the ambient *ext*BC (Fig. 3). In the mobility diameter range of 140–750 nm, the fitted D_f is 2.36, with one standard deviation of 0.04. It is comparable with the D_f values of diesel exhaust particles. For example, depending on the fuel type, engine type and load, the D_f of diesel exhaust particles measured by the DMA-APM or DMA-ELPI system ranged between 2.22 and 2.84 (Park et al., 2003; Maricq and Xu, 2004; Olfert et al., 2007). This similarity indicates the dominant contribution of diesel exhausts to the *ext*BC in our measurement site in urban Beijing. A high fraction of organic and/or inorganic (e.g., sulfate) components in the diesel exhausts increased the D_f values by filling in the gap of the chain-like agglomerates or coatings outside the primary spherules (Park et al.,2003; Olfert et al., 2007). Thus, the relatively low D_f value observed in urban Beijing is likely related to the high fuel quality (e.g., low sulfur content) and more efficient combustion in the vehicle engines, which decrease the organic and/or inorganic fractions in diesel exhausts. The D_f value for the ambient soot agglomerates measured with a DMA-APM system near a diesel truck-dominated highway was 2.41 (Geller et al., 2006), very close to the value in our study.

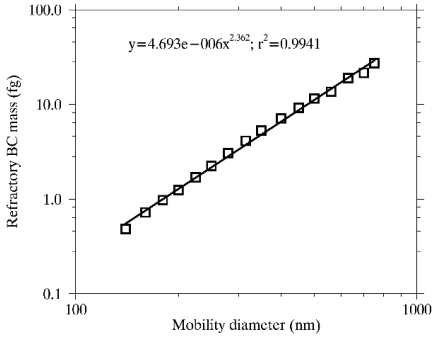

Fig. 3 The mass of *ext*BC particles as a function of the mobility diameter (gray squares),

Atmos. Meas. Tech. Discuss., https://doi.org/10.5194/amt-2018-408
Manuscript under review for journal Atmos. Meas. Tech.
Discussion started: 10 December 2018

Atmospheric Measurement Techniques Discussions

fitted by a power law relationship (black line).

Fig. 4 shows the diurnal variation of D_f. A significant low value of D_f (2.25±0.05) was observed in the morning traffic rush hours (06:00–09:00 local time). Freshly emitted *ext*BC particles from vehicle exhaust have a looser chain-like structure corresponding to a low D_f value. The highest D_f value (2.38±0.06) in the afternoon (12:00–15:00 local time) is likely related to the aging processes of the *ext*BC particles in the ambient atmosphere. Aging processes not only result in a higher fraction of *int*BC particles (Wu et al., 2016, 2017) but they can also lead to a more compact structure of *ext*BC particles, and in turn, a higher D_f value. BC particles thinly-coated by organic/inorganic components were somewhat considered as *ext*BC using the SP2 time delay approach (Moteki and Kondo, 2007; Laborde et al., 2012). However, less mass condensed onto the BC primary particles would lead to more compaction of the *ext*BC particles even when the d_{mob} remained constant (Slowik et al., 2007).

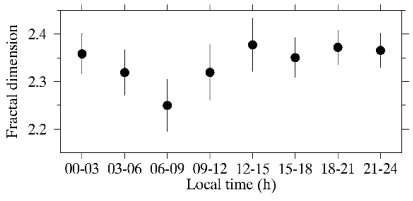

Fig. 4 The diurnal variation of the fractal dimension (D_f) of ambient *ext*BC particles. The error bars represent one standard deviation of the fitted D_f.

4.2 Size-resolved effective densities of the ambient *ext*BC

In contrast to the mass of *ext*BC (m), the effective density of the *ext*BC particles (ρ_{eff}) showed a significant decreasing trend as d_{mob} increased from 140 nm to 750 nm (Fig. 5). The highest ρ_{eff} of 0.34 g cm^{-3} was observed in the d_{mob} range of 140–160 nm, likely due to the fewest primary spherules of the BC aggregates at the smallest size. When d_{mob} increased to 700 nm, ρ_{eff} decreased to as low as 0.12 g cm^{-3}, approximately one-third of that at 140–160 nm. The very low ρ_{eff} values agree well with the fractal-like nature of the *ext*BC particles.

Atmos. Meas. Tech. Discuss., https://doi.org/10.5194/amt-2018-408
Manuscript under review for journal Atmos. Meas. Tech.
Discussion started: 10 December 2018

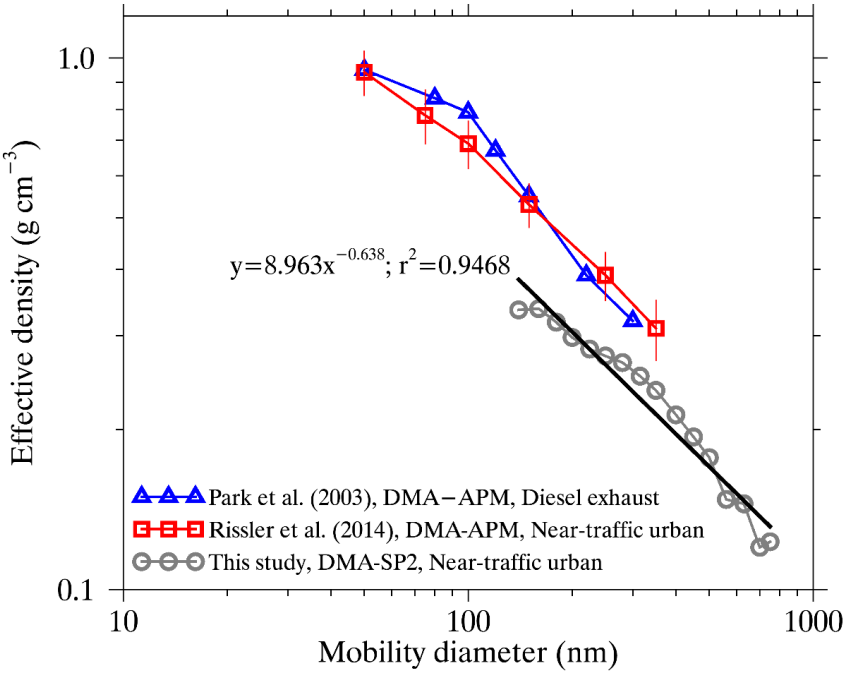

Fig. 5 The effective density (ρ_{eff}) of the *ext*BC particles as a function of mobility diameter (d_{mob}) (gray cycles). The black line represents the power law fitting of ρ_{eff} against d_{mob}. The variations of ρ_{eff} with d_{mob} measured for the soot agglomerates from diesel exhausts (Park et al., 2003) and near-traffic urban environments (Rissler et al., 2014) are also presented as blue triangles and red squares, respectively.

The ρ_{eff} values measured with the DMA-SP2 measurement are considerably lower than those of diesel exhaust particles measured by the DMA-APM or DMA-ELPI systems. Park et al. (2003) reported a decrease in ρ_{eff} of diesel exhaust particles under a 50% engine load from 0.95 g cm^{-3} to 0.32 g cm^{-3} as the mobility diameter increased from 50 nm to 300 nm (Fig. 5). The ρ_{eff} values presented in Park et al. (2003) are approximately 1.62, 1.34 and 1.23 times those in our study at ~150 nm, 220 and 300 nm in mobility diameter, respectively. Some previous studies on the ρ_{eff} of diesel exhaust particles also commonly showed a larger ρ_{eff} than that measured in this study (Maricq and Xu, 2004; Olfert et al., 2007). Nevertheless, the ρ_{eff} values reported in the literature also differ. For

example, Olfert et al. (2007) found that the ρ_{eff} of diesel exhaust particles coated with little sulfate and water content was ~0.4 g cm^{-3} at 299 nm, larger than the value of 0.32 g cm^{-3} in Park et al. (2003) and 0.26 g cm^{-3} in our study for the same mobility size. The ρ_{eff} of ambient soot aggregates also showed a similar decreasing trend with increasing d_{mob} based on the DMA-APM system (Geller et al., 2006; Rissler et al., 2014). Rissler et al. (2014) showed a decrease in the average ρ_{eff} of BC aggregates from 0.94 g cm^{-3} to 0.31 g cm^{-3} in the near-traffic urban environment as d_{mob} increased from 50 nm to 350 nm (Fig. 5), similar to that of the freshly emitted diesel exhaust particles presented in Park et al. (2003). However, based on the same method, the ρ_{eff} values of the ambient BC aggregates that mostly originated from diesel exhausts (Geller et al., 2006) are largely different from those presented in Rissler et al. (2014), especially in the large particle size range. The ρ_{eff} at ~350 nm was 0.17 g cm^{-3} in Geller et al. (2006), approximately half of the value presented in Rissler et al. (2014). The reason for the discrepancy might be related to the large measurement uncertainties of the DMA-APM system for large particles, e.g., with sizes greater than 300 nm in d_{mob}, since these large particles are less abundant in the ambient atmosphere (Geller et al., 2006).

The DMA-APM system directly measures the mass of particles selected at a given mobility diameter by the DMA. The organic and/or inorganic components filling in the gap or coating outside the primary spherules will increase the mass of the BC agglomerates, although their content might not be significant in fresh exhausts. Olfert et al. (2007) showed that sulfates and water accounted for ~2% of the mass of the total particulate matter under a low engine load (15%) and increased to ~30% under a high engine load (40%). Rissler et al. (2014) found that the volatile mass fraction of the soot aggregate was ~10% when heated to 300 °C. Thus, in practice, the DMA-APM system measured the ρ_{eff} of soot particles comprising chain-like BC aggregates and a few volatile components instead of pure BC. However, the SP2 measured the mass of pure BC merely through its incandescence in the laser beam, and the DMA-SP2 system determined the ρ_{eff} of *ext*BC exclusive of those volatile components coupled in the BC particles. Thus, a lower ρ_{eff} was obtained, but this value was likely closer to the value of the pure *ext*BC particles.

Atmos. Meas. Tech. Discuss., https://doi.org/10.5194/amt-2018-408
Manuscript under review for journal Atmos. Meas. Tech.
Discussion started: 10 December 2018

Atmospheric Measurement Techniques Discussions

Although the ρ_{eff} of *ext*BC at small sizes (d_{mob}<140 nm) cannot be determined due to the limitation of the DMA-SP2 system, we extended the ρ_{eff} of *ext*BC to a large size range (300<d_{mob}<750), which was barely investigated in previous studies. A continuous decrease in ρ_{eff} with increasing d_{mob} was observed even in the large size range between 300 nm and 750 nm (Fig. 5). It is reasonable that the structure of the *ext*BC particles is looser when the agglomerate chain built up by the primary spherules increases.

4.3 Dynamic shape factors of the ambient *ext*BC

Due to the chain-like structures, the *ext*BC particles generally have large dynamic shape factors (χ) with values in the range of 2.53 to 3.18, much larger than that of *int*BC with an average value of ~1.2 (Zhang et al., 2016). In general, the χ values are significantly higher for larger particle sizes. The *ext*BC particles 700 nm in mobility diameter have a mean χ value of 3.18, approximately 1.26 times that for 160 nm particles. The larger particles have longer chains and looser structures, resulting in higher χ values. However, the χ values varied slightly, fluctuating in a narrow range between 2.53 to 2.64 in the size range of 140 nm to 350 nm. This is attributed to the large drag force for smaller particles.

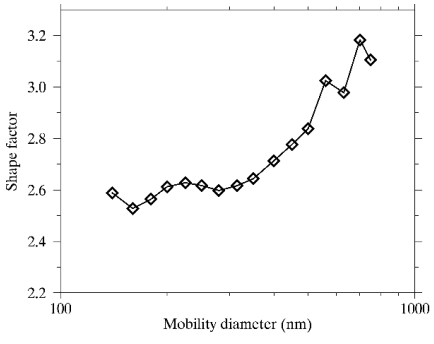

Fig. 6 The dynamic shape factor of the *ext*BC particles as a function of the mobility diameter.

5 Conclusion

The DMA-SP2 system was established to study the morphology of the ambient *ext*BC

particles. The quasi-monodisperse particles in the d_{mob} range of 20–750 nm were stepwise selected using the DMA and then delivered to the SP2 for BC mass measurement and mixing state discrimination. The time difference between the size selection and the SP2 measurement was previously processed using the local peak approach. Gaussian fitting was performed to the *ext*BC mass frequency distribution to minimize the effect of multicharged particles and obtain the typical *ext*BC mass at a given d_{mob}. On this basis, the D_f was estimated to be 2.36±0.04 by fitting the derived *ext*BC masses against d_{mob} in the range of 140–750 nm, close to the D_f values of diesel exhaust particles. A relatively lower D_f value was observed in the morning traffic rush hours, implying a significant contribution of vehicle emissions to the agglomerate BC particles. A decrease in ρ_{eff} with increasing d_{mob} was observed, with the ρ_{eff} value decreasing from 0.34 g cm^{-3} at 140–160 nm to 0.12 g cm^{-3} at 700 nm. The ρ_{eff} values derived using the DMA-SP2 measurement were generally lower than those based on the DMA-APM measurement. This was most likely due to the bias in the *ext*BC mass determination between the SP2 and APM. The pure refractory BC mass determined using the SP2 in this study was generally lower than the mass of the BC aggregate, which comprises both refractory BC and nonrefractory organic and/or inorganic components. The large χ values varying in the range of 2.53 to 3.18 were derived at different d_{mob}, further implying the high fractal structure of *ext*BC particles.

Acknowledgements

This work was supported by the National Key Research and Development Program of China (no. 2017YFC0209601, 2017YFC0212701) and the National Natural Science Foundation of China (no. 41575150, 41775155, 91644217 and 91644219).

References

Alexander, D. T., Crozier, P. A., and Anderson, J. R.: Brown carbon spheres in East Asian outflow and their optical properties, Science, 321, 833–836, doi:10.1126/science.1155296, 2008.

Huang, X. F., Sun, T. L., Zeng, L. W., Yu, G. H., and Luan, S. J.: Black carbon aerosol characterization in a coastal city in South China using a single particle soot photometer, Atmos. Environ., 51, 21–28, doi:10.1016/j.atmosenv.2012.01.056, 2012.

396 Geller, M., Biswas, S., and Sioutas, C.: Determination of particle effective density in urban environments with a
397 differential mobility analyzer and aerosol particle mass analyzer, Aerosol Sci. Technol., 40, 709–723,
398 doi:10.1080/02786820600803925, 2006.
399 Gysel, M., Laborde, M., Olfert, J. S., Subramanian, R., and Gröhn, A. J.: Effective density of Aquadag and fullerene
400 soot black carbon reference materials used for SP2 calibration, Atmos. Meas. Tech., 4, 2851–2858,
401 doi:10.5194/amt-4-2851-2011, 2011.
402 IPCC: Summary for policymakers, in: Climate Change 2013: The Physical Science Basis. Contribution of Working
403 Group I to the Fifth Assessment Report of the Intergovernmental Panel on Climate Change, edited by: Stocker,
404 T. F., Qin, D., Plattner, G.-K., Tignor, M., Allen, S. K., Boschung, J., Nauels, A., Xia, Y., Bex, V., and Midgley,
405 P. M., Cambridge University Press, Cambridge, United Kingdom and New York, NY, USA, 2013.
406 Jacobson, M. Z.: Strong radiative heating due to the mixing state of black carbon in atmospheric aerosols, Nature,
407 409, 695–697, doi:10.1038/35055518, 2001.
408 Khalizov, A. F., Xue, H. X., Wang, L., Zheng, J., and Zhang, R. Y.: Enhanced light absorption and scattering by
409 carbon soot aerosol internally mixed with sulfuric acid, J. Phys. Chem. A, 113, 1066–1074, 2009.
410 Laborde, M., Mertes, P., Zieger, P., Dommen, J., Balternsperger, U., and Gysel, M.: Sensitivity of the Single Particle
411 Soot Photometer to different black carbon types, Atmos. Meas. Tech., 5, 1031–1043, doi:10.5194/amt-5-1031-
412 2012, 2012.
413 Liu, D. T., Whitehead, J., Alfarra, M. R., Reyes-Villegas, E., Spracklen, D. V., Reddington, C. L., Kong, S. F.,
414 Williams. P. I., Ting, Y.-C., Haslett, S., Taylor, J. W., Flynn, M. J., Morgan, W. T., McFiggans, G., Coe, H., and
415 Allan, J. D.: Black-carbon absorption enhancement in the atmosphere determined by particle mixing state,
416 Nature Geoscience, 10, 184–188, doi:10.1038/NGEO2901, 2017.
417 Maricq, M. M., and Xu, N.: The effective density and fractal dimension of soot particles from premixed flames and
418 motor vehicle exhaust, J. Aerosol Sci., 35, 1251–1274, doi:10.1016/j.jaerosci.2004.05.002, 2004.
419 McMeeking, G. R., Good, N., Petters, M. D., McFiggans, G., and Coe, H.: Influences on the fraction of hydrophobic
420 and hydrophilic black carbon in the atmosphere, Atmos. Chem. Phys., 11, 5099–5112, doi:10.5194/acp-11-
421 5099-2011, 2011.
422 Moteki, N. and Kondo, Y.: Effects of mixing state on black carbon measurements by laser-induced incandescence,
423 Aerosol Sci. Technol., 41, doi:10.1080/02786820701199728, 398–417, 2007.
424 Ning, Z., Chan, K. L., Wong, K. C., Westerdahl, D., Močnik, G., Zhou, J. H., Cheung, C. S.: Black carbon mass size
425 distributions of diesel exhaust and urban aerosols measured using differential mobility analyzer in tandem with
426 Aethalometer, Atmos. Environ., 80, 31–40, doi:10.1016/j.atmosenv.2013.07.037, 2013.
427 Olfert, J. S., Symonds, J. P. R., and Collings, N.: The effective density and fractal dimension of particles emitted
428 from a light-duty diesel vehicle with a diesel oxidation catalyst, J. Aerosol Sci., 38, 69–82,
429 doi:10.1016/j.jaerosci.2006.10.002, 2007.
430 Pagels, J., Khalizov, A. F., McMurry, P. H., and Zhang, R. Y.: Processing of soot by controlled sulphuric acid and
431 water condensation—mass and mobility relationship, Aerosol Sci. Technol., 43, 629–640,
432 doi:10.1080/02786820902810685, 2009.
433 Park, K., Cao, F., Kittelson, D. B., and McMurry, P. H.: Relationship between particle mass and mobility for diesel
434 exhaust particles, Environ. Sci. Technol., 37, 577–583, doi:10.1021/es025960v, 2003.
435 Park, K., Kittelson, D. B., and McMurry, P. H.: Structural properties of diesel exhaust particles measured by
436 transmission electron microscopy (TEM): relationships to particle mass and mobility, Aerosol Sci. Technol.,
437 38, 881–889, doi:10.1080/027868290505189, 2004.
438 Park, K., Dutcher, D., Emery, M., Pagels, J., Sakurai, H., Scheckman, J., Qian, S., Stolzenburg, M. R., Wang, X.,
439 Yang, J., and McMurry, P. H.: Tandem measurements of aerosol properties—a review of mobility techniques

with extensions, Aerosol Sci. Technol., 42, 801–816, doi:10.1080/02786820802339561, 2008.

Peng, J. F., Hu, M., Guo, S., Du, Z. F., Zheng, J., Shang, D. J., Zamora, M. L., Zeng, L. M., Shao, M., Wu, Y.-S., Zheng, J., Wang, Y., Glen, C. R., Collins, D. R., Molina, M. J., and Zhang, R. Y.: Markedly enhanced absorption and direct radiative forcing of black carbon under polluted urban environments, Proc. Natl. Acad. Sci. USA, 113, 4266–4271, doi:10.1073/pnas.1602310113, 2016.

Rissler, J., Nordin, E. Z., Eriksson, A. C., Nilsson, P. T., Frosch, M., Sporre, M. K., Wierzbicka, A., Svenningsson, B., Löndahl, J., Messing, M. E., Sjogren, S., Hemmingsen, J. G., Loft, S., Pagels, J. H., and Swietlicki, E.: Effective density and mixing state of aerosol particles in a near-traffic urban environment, Environ. Sci. Technol., 48, 6300–6308, doi:10.1021/es5000353, 2014.

Seinfeld, J. H., and Pandis, S. N.: Atmospheric chemistry and physics, Chapter 9–Dynamics of single aerosol particles, John Wiley & Sons, Inc., Hoboken, New Jersey, 2006.

Schwarz, J. P., Gao, R. S., Fahey, D. W., Thomson, D. S., Watts, L. A., Wilson, J. C., Reeves, J. M., Darbeheshti, M., Baumgardner, D. G., Kok, G. L., Chung, S. H., Schulz, M., Hendricks, J., Lauer, A., Kärcher, B., Slowik, J. G., Rosenlof, K. H., Thompson, T. L., Langford, A. Q., Loewenstein, M., and Aikin, K. C.: Single-particle measurements of midlatitude black carbon and light-scattering aerosols from the boundary layer to the lower stratosphere, J. Geophys. Res., 111, D16207, doi:10.1029/2006JD007076, 2006.

Schwarz, J. P., Gao, R. S., Spackman, J. R., Watts, L. A., Thomson, D. S., Fahey, D. W., Ryerson, T. B., Peischl, J., Holloway, J. S., Trainer, M., Frost, G. J., Baynard, T., Lack, D. A., de Gouw, J. A., Warneke, C., and Del Negro, L. A.: Measurement of the mixing state, mass, and optical size of individual black carbon particles in urban and biomass burning emissions, Geophys. Res. Lett., 35, L13810, doi:10.1029/2008GL033968, 2008.

Shiraiwa, M., Kondo, Y., Iwamoto, T., and Kita, K.: Amplification of light absorption of black carbon by organic coating, Aerosol Sci. Technol., 44, 46–54, doi:10.1080/02786820903357686, 2010.

Slowik, J. G., Cross, E. S., Han, J. H., Kolucki, J., Davidovits, P., Williams, L. R., Onasch, T. B., Jayne, J. T., Kolb, C. E., and Worsnop, D. R.: Measurements of morphology changes of fractal soot particles using coating and denuding experiments: implications for optical absorption and atmospheric lifetime, Aerosol Sci. Technol., 41, 734–750, doi:10.1080/02786820701432632, 2007.

Wang, Q. Y., Huang, R. J., Cao, J. J., Han, Y. M., Wang, G. H., Li, G. H., Wang, Y. C., Dai, W. T., Zhang, R. J., and Zhou, Y. Q.: Mixing state of black carbon aerosol in a heavily polluted urban area of China: implications for light absorption enhancement, Aerosol Sci. Technol., 48, 689–697, doi:10.1080/02786826.2014.917758, 2014.

Wentzel, M., Gorzawski, H., Naumann, K.-H., Saathoff, H., and Weinbruch, S.: Transmission electron microscopical and aerosol dynamical characterization of soot aerosols, J. Aerosol Sci., 34, 1347–1370, doi:10.1016/S0021-8502(03)00360-4, 2003.

Wu, Y. F., Zhang, R. J., Tian, P., Tao, J., Hsu, S.-C., Yan, P., Wang, Q. Y., Cao, J. J., Zhang, X. L., and Xia, X. A.: Effect of ambient humidity on the light absorption amplification of black carbon in Beijing during January 2013, Atmos. Environ., 124, 217–223, doi:10.1016/j.atmosenv.2015.04.041, 2016.

Wu, Y. F., Wang, X. J., Tao, J., Huang, R. J., Tian, P., Cao, J. J., Zhang, L. M., Ho, K.-F., Han, Z. W., and Zhang, R. J.: Size distribution and source of black carbon aerosol in urban Beijing during winter haze episodes, Atmos. Chem. Phys., 17, 7965–7975, doi:10.5194/acp-17-7965-2017, 2017.

Zhang, R. Y., Khalizov, A. F., Pagels, J., Zhang, D., Xue, H., Chen, J., and McMurry, P. H.: Variability in morphology, hygroscopic and optical properties of soot aerosols during internal mixing in the atmosphere, Proc. Natl. Acad. Sci. USA, 105, 10291–10296, doi:10.1073/pnas.0804860105, 2008.

Zhang, Y. X., Zhang, Q., Cheng, Y. F., Su, H., Kecorius, S., Wang, Z. B., Wu, Z. J., Hu, M., Zhu, T., Wiedensohler, A., and He, K. B.: Measuring the morphology and density of internally mixed black carbon with SP2 and VTDMA: new insight into the absorption enhancement of black carbon in the atmosphere, Atmos. Meas. Tech.,

Atmos. Meas. Tech. Discuss., https://doi.org/10.5194/amt-2018-408
Manuscript under review for journal Atmos. Meas. Tech.
Discussion started: 10 December 2018

Atmospheric Measurement Techniques Discussions

484 9, 1833–1843, doi:10.5194/amt-9-1833-2016, 2016.